# Modeling of Animal Vibrissae: Adaptive Control of Multi-body Systems under Output Noise

1st Carsten Behn
*Schmalkalden University of Applied Sciences*
Schmalkalden, Germany
c.behn@hs-sm.de
https://orcid.org/0000-0001-7618-1926

2nd Moritz Scharff
*Wilhelm-Franke-Str. 11*
Dresden, Germany
moritz.scharff@live.de
https://orcid.org/0000-0002-1581-7668

3rd Lukas Merker
*Technische Universität Ilmenau*
Ilmenau, Germany
lukas.merker@tu-ilmenau.de
https://orcid.org/0000-0003-1931-0749

***Abstract*—The reception of vibrations is a special sense of touch, important for many insects and vertebrates. The latter realize this reception by means of hair-shaped vibrissae all over the body, but especially arranged in the mystacial pad around the snout. Latest research activities focus on modeling these sensor components to explain some biological behaviors/features (Technical Biology) or to investigate their usage for technical applications for, e.g., object surface and/or shape detection (Bionics). In contrast to these works, we focus on the modeling of the dynamic operation modes to be applied for dynamic scanning patterns of objects. We set up a principal mechanical model of a single vibrissa to describe these modes of operation: passive and active vibrissae. They are either used passively to sense environmental forces, e.g., wind, or actively, when they are rhythmically moved to scan objects or surfaces. Consequently, the vibrissa inspired model has to allow for stabilizing and tracking control as well, but yet being able to detect (superimposed) solitary excitations. Hence, the biological paradigm exhibits some adaptive behavior, and so must the controller: to be adaptive in view of both the randomness of the external signals to be suppressed and the uncertainty of the system data.**

***Index Terms*—vibrissa; modes of operation; adaptive control; uncertain system; tactile sensor**

## I. Introduction

Tactile sensor technology seems nowhere near from playing a key role in environmental exploration in mobile robotics, especially when compared to optical sensing technology. Taking a glance at the world of biology, the sense of touch provides necessary information for several species, e.g., mammals, especially nocturnal animals like rats. They exhibit a sophisticated tactile sense organ supporting tactile exploration which complements the visual and aural sensing: the mystacial vibrissae in the snout region, see Fig. 1.

Fig. 1. Mammals with vibrissae: a cat named 'Alfred' with whiskers (left), and a rat (right) [3].

The rats benefit from their vibrissae in different ways while they are moved in different modes of operation [1], [2]: they are involved in their social behavior, acquisition of food, locomotion, navigation [4], [5], detecting air flows [6]. They enable the rats to detect, localize and recognize objects near their faces [7], including detection of object features (orientation, shape, texture) [8], [9].

The mystacial vibrissae are arranged in an array of columns and rows around the snout, see Fig. 2.

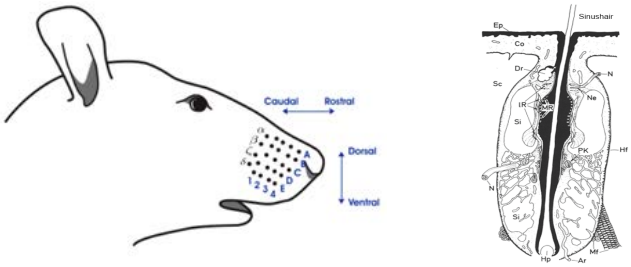


Fig. 2. Schematic drawing of the mystacial pad (left) [10], follicle-sinus-complex of a vibrissa (right) [11].

The vibrissa itself (made of dead material) is mainly used as a lever for the force transmission. But, in contrast to ordinary hairs, vibrissae are stiffer and have a hollow conical shape [10]. Each vibrissa in the mystacial pad is embedded in and supported by its own follicle-sinus complex (FSC), see Fig. 2, right. The FSC is characterized by its exceptional arrangement of blood vessels, neural bonding and muscles.

Despite the distribution and difference of the vibrissae in a mystacial pad with respect to their (varying) material and geometrical features (multi-layer system, slenderness, conical shape with inherent curvature inside this pad), we focus on a single vibrissa, its surrounding tissue, its functionality and mode of operation. For a more detailed overview see [12]. Due to [13], the surrounding musculature is divided in extrinsic and intrinsic one. The vibrissa can either be moved passively (e.g., by wind), or actively through alternate contractions of the intrinsic and extrinsic muscles. The resulting rhythmic pro- and retractions of the vibrissa, called whisking, are used to scan surfaces and objects [11]. Relevant information can be perceived by adjusting the frequency and amplitude of

the oscillation to each task. By observing rats accomplishing several types of exercises, Berg and Kleinfeld in [14] could distinguish two main *whisking patterns*: *exploratory whisking* when rodents explore their environment with large amplitude sweeps in a low frequency (5-15Hz) range, and *foveal whisking* when rodents palpate object surfaces with small amplitude, high frequency (15-25Hz) movements. Summarizing, the complex FSC- and muscle-system enables the rodents to use their vibrissae in two different ways (modes of operation):

- In the **passive mode**, the vibrissae are being deflected by external forces (e.g., wind). They return to their rest position passively — thus without any muscle activation.
- In the **active mode**, the vibrissae are swung back- and forward by alternate contractions of the intrinsic and extrinsic muscles. By adjusting the frequency and amplitude of the oscillations, the rodents are able to investigate object surfaces and shapes amazingly fast and with high precision [15].

But, how the animals convert these multiple contacts with single objects into coherent information about their surroundings remains unclear and is not of focus in this work. However, from the point of view from control theory, every biological sensory system has the ability to constantly adapt its sensitivity to its current environment in a way that empowers it to distinguish the relevant information out of the multitude of negligible stimuli ($\rightarrow$ *adaptive system*). Several *control strategies* enhance the relevance-oriented stimulus processing:

- a feedback-loop (closed-loop control system) enables the rodents to immediately react to an object contact: they slow down the concerned vibrissae, diminishing the occurring wear-out effect on the hair [16], [17],
- depending on the mode (passive or active) and the expectations of the rodent, the neurons reaction is being suppressed, enhanced or left unaltered [18]–[20].

Therefore, this biological sensor system is highly interesting for applications in the field of autonomous robotics, since tactile sensors can offer reliable information, where conventional sensors fail (in dark, smoky or noisy environments).

In the following Section II, we give a very brief overview on mathematical models to describe the rigid-body motion of vibrissa-like mechanical systems. In Section III, we set up a simple model of a single vibrissa, derive the equations of motion for a stringent mathematical treatment. For this, we present some aspects of control theory for this systems in Section IV. We introduce a general system class this equations of motion belongs to and show some output feedback controllers mimicking the adaptive nature of the mentioned different modes of operation of a vibrissa. Numerical simulations in Section V show the effectiveness of these controllers in $\lambda$-tracking some reference signals such that the system is in a passive or active mode. The main difference to [1] is presented in Section VI, where we –additionally to new adaptors– focus on noise-corrupted outputs due to some measurement failures and show that the suggested adaptive tracking strategies still work effectively. Section VII concludes the paper and closes with an outlook.

## II. State of the art - Modeling animal vibrissae

An intensive literature overview of technical vibrissa models (rigid body and continuum) has been presented in [21]–[23]. Here, we briefly discuss some models therein, where we restrict the investigations to rigid body models, continuous models are in recent exploration.

The following summarizes the relevant information of the encountered mechanical models found in the literature for this paper.

- Mitchinson in 2004 [24] and 2007 [17] - *Model of the FSC*: Mitchinson's research group has developed a model of the FSC to increase the knowledge over this biological sensory system on the one hand, and on the other hand to promote the development of innovative and efficient tactile sensors. Following the anatomy in literature, the scientists modeled the various layers of the FSC, linking them with spring and damping elements to simulate the compliance of the biological tissue (see Fig. 3).

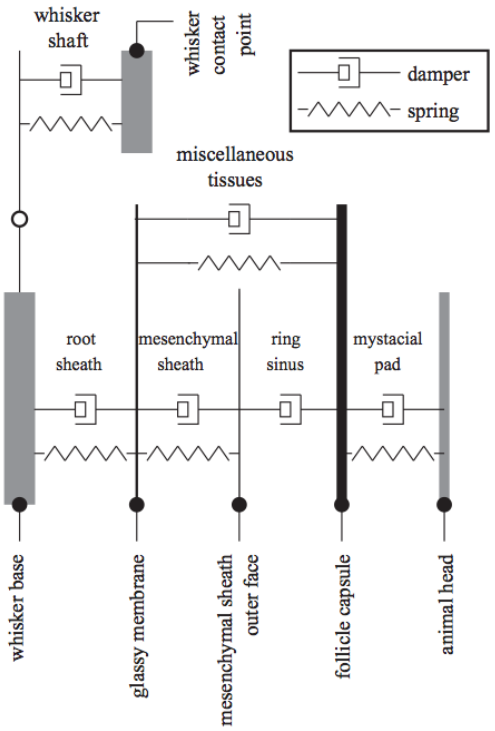


Fig. 3. Mechanical model of the FSC of [24].

  - ⊖ too complex for a technical implementation
  - ⊕ Determination of spring and damping coefficients for the FSC
- Berg in 2003 [14] - *Determination of the range of movement of the vibrissa*: The function of the musculature in the mystacial pad was investigated by Berg and Hill in [14]. They recorded electromyogram (EMG) activity from the intrinsic and extrinsic muscles while rats were

whisking, to characterize the pattern of muscular dynamics. The following observations were made during one whisking cycle, also see Fig. 4:

- the **protraction** of the vibrissa is caused by the contraction of the intrinsic muscle retracting the FSC ($\rightarrow$ **angular deflection**),
- the **retraction** of the vibrissa is induced by the contraction of the extrinsic muscle retracting the vibrissa at skin level ($\rightarrow$ **translatory shift**).

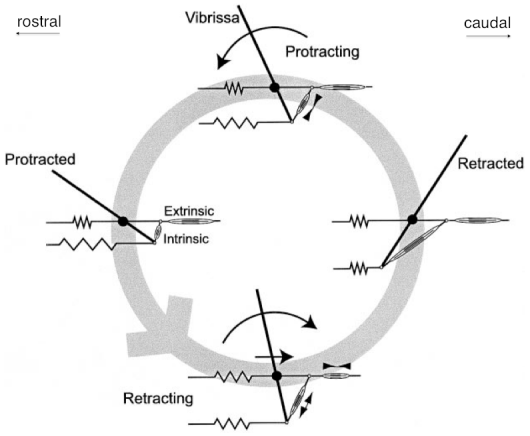


Fig. 4. Mechanical model relating cyclic vibrissa movements according to alternating intrinsic and extrinsic muscle contractions during whisking of [14].

Summarizing:

$\hookrightarrow$ $\varphi_{Rest} \approx 80°$
hence: angular deflection in rostral direction $\varphi_{rest} + 65°$, angular deflection in caudal direction $\varphi_{rest} - 35°$, translatory shift $\approx 5mm$ in caudal-rostral direction, translatory shift $\approx 3mm$ in dorsal-ventral direction

- Hill in 2008 [25] - *Model of the musculature in the mystacial pad*: The researchers developed a mechanical model of the vibrissa, focussing on the relationship between the various muscle contractions and the resulting vibrissa motion. Furthermore, three vibrissa / follicle units, linked by spring and damping elements, were incorporated in the model so that the influence of the intrinsic muscle slings on their neighboring follicles could also be considered, see Fig. 5.
  The fact that a passively deflected vibrissa returns to its initial position without oscillating, implies that the mystacial pad is overdamped. Summarizing:
  - $\oplus$ Implementation of intrinsic and extrinsic musculature
  - $\oplus$ Simulating the viscoelastic properties of the skin
    $\hookrightarrow$ Determination of spring and damping coefficients for the skin
  - $\ominus$ Negligence of the viscoelastic properties of the FSC
  - $\ominus$ Connection between the follicles
    $\hookrightarrow$ leads to complex control strategy and high control effort

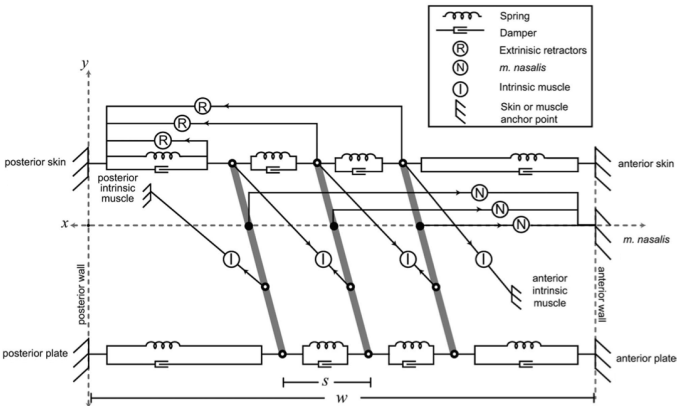


Fig. 5. Schematic drawing of the mechanical model of a row of three vibrissae in [25].

- models by Simony [26] and Haiderliu [27] in 2010 are too complex in their structure and neglected for discussion here
- Behn in 2013 [22] - *Model of stimulus transmission*
  - $\oplus$ Implementation of viscoelastic properties of FSC
  - $\ominus$ Negligence of the viscoelastic properties of the skin

The goal is *not* to recreate an exact copy of the biological system, but *to implement the specific characteristics of the vibrissa needed for the detection of useful information in challenging surroundings in a mechanical model.* Principally, the tenor of our investigations is from bionics: modeling live paradigms, exploiting corresponding mathematical models in order to understand details of internal processes and, possibly, coming to artificial prototypes (e.g., sensors in robotics). We point out that we focus on a single vibrissa and not on a tuft of various vibrissae as in [27].

## III. A FIRST MODEL OF A SINGLE VIBRISSA

In this section, we present a first vibrissa-inspired sensor model and derive the corresponding equations of motion.

Following [13] and as mentioned in Section I, the vibrissa is supported by its FSC. Important parts of it are an enveloping chamber with controllable blood supply, and intrinsic and extrinsic muscles which control the vibrissa motions. This biological description suggests physical models as sketched in Fig. 6, and these then lead us to the mathematical model based on the pendulum device in Fig. 7.

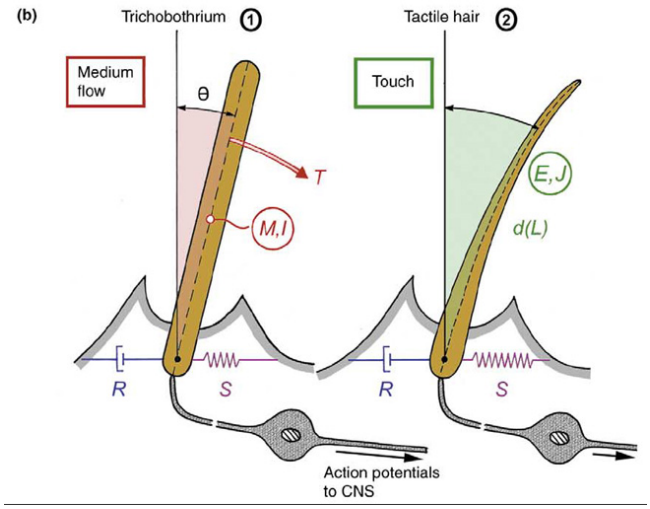


Fig. 6. Scheme of a vibrissa, [28].

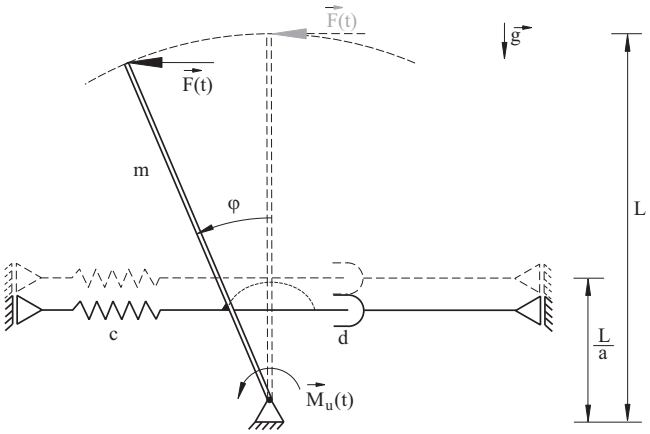


Fig. 7. A mechanical model of a vibrissa.

The model has a viscoelastic support (skin level) and is acted upon by a force excitation $F(\cdot)$ and a control torque $M_u(\cdot)$. The control torque is due to control impact by the musculature [13]. The equations of motion are given by the Principle of Angular Momentum:

$$J_0\,\ddot{\varphi}(t) = \frac{L}{2}\,m\,g\,\sin\big(\varphi(t)\big) - \frac{L^2}{a^2}\,c\,\sin\big(\varphi(t)\big)\,\cos\big(\varphi(t)\big) - \frac{L^2}{a^2}\,d\,\cos\big(\varphi(t)\big)^2\,\dot{\varphi}(t) + L\,\cos\big(\varphi(t)\big)\,F(t) + M_u(t)\,, \quad (1)$$

where $J_0 := \frac{1}{3}\,m\,L^2$ is the moment of inertia about the pivot. The output of the system is $y(t) = \varphi(t)$.

## IV. Mathematical Background

Dealing with sophisticated, biologically inspired systems, one cannot expect to have all information about it. Instead only structural properties are known. In doing so, we assume that internal data (e.g., mass, spring stiffness, and damping ratio) are unknown. Furthermore, with respect to a changing, and therefore uncertain, environment, we assume the external excitations to be unknown which leads us to the treatment of *highly uncertain (control) system* of known structure given in (1). Note that this system belongs to the following general system class, firstly presented in [22]: finite-dimensional, nonlinearly perturbed, $m$-input $u(\cdot)$, $m$-output $y(\cdot)$ systems (MIMO-system) of relative degree two with known sign of the high-frequency gain $G$:

$$\begin{aligned} \ddot{y}(t) &= A_1\,\dot{y}(t) + f_1(s_1(t), y(t), z(t)) + G\,u(t)\,, \\ \dot{z}(t) &= A_2\,z(t) + A_3\,\dot{y}(t) + f_2(s_2(t), y(t))\,, \end{aligned} \quad (2)$$

with initial conditions $y(t_0) = y_0 \in \mathbb{R}^m$, $\dot{y}(t_0) = y_1 \in \mathbb{R}^m$ and $z(t_0) = z_0 \in \mathbb{R}^{n-2m}$ and the following properties:

- dimensions $u(t) \in \mathbb{R}^m$, $A_1$, $G \in \mathbb{R}^{m\times m}$, $A_2 \in \mathbb{R}^{(n-2m)\times(n-2m)}$ and $A_3 \in \mathbb{R}^{(n-2m)\times m}$, $n \geq 2m$,
- spectrum$(G) \subset \mathbb{C}_+$, i.e., the spectrum of the high-frequency gain lies in the open right-half complex plane,
- $s_1 \in \mathcal{L}^\infty(\mathbb{R}_{\geq 0}, \mathbb{R}^q)$ and $s_2 \in mathcalL^\infty(\mathbb{R}_{\geq 0}, \mathbb{R}^q)$ can be thought of (bounded) disturbance terms, whereby $\mathcal{L}^\infty(\mathbb{R}_{\geq 0}, \mathbb{R}^q)$ is the space of measurable essentially bounded functions with infinity-norm, see [29],
- $f_1 : \mathbb{R}^q \times \mathbb{R}^m \times \mathbb{R}^{n-2m} \to \mathbb{R}^m$ and $f_2 : \mathbb{R}^q \times \mathbb{R}^m \to \mathbb{R}^{n-2m}$ are continuous and linearly affine bounded functions,
- spectrum$(A_2) \subset \mathbb{C}_-$, i.e., the spectrum of the high-frequency gain lies in the open left-half complex plane, which equals that the system is minimum phase, provided $f_1 \equiv 0$ and $f_2 \equiv 0$.

Using these descriptions, the reader can easily identify the components of (1) in the explanations given above. Some assertions are given in a more general way than presented in the equation of motion (1) to encompass more systems, which can be $\lambda$-tracked later in this paper.
Relative degree two means that the input $u$ directly influences the second derivative of each output component.

To dominate this system with uncertain parameters, we have to design an adaptive controller which learns from the behavior of the system in automatically adjusting its (gain) parameters to achieve a desired control objective. Because the system is excited by unknown forces (e.g., possible wind from the environment), we try to design a universal feedback controller which adaptively compensates this unknown excitation and leaves the system in a desired operation pattern.

Since we are dealing with an uncertain, randomly perturbed, non-autonomous system, particular attention is paid to the adaptive $\lambda$-*tracking control objective*: determine a universal $\lambda$-controller, which learns from the behavior of the system and automatically adjusts its parameters such that the system tracks a given reference signal $y_{\text{ref}}(\cdot)$ (representing a desired mode of operation) with a prescribed accuracy $\lambda$. The value $\lambda > 0$ denotes the size of the feasible tracking error, which means that the error $e(t) := y(t) - y_{\text{ref}}(t)$ is forced, via the adaptive feedback mechanism, towards a ball around zero of arbitrary

small pre-specified radius $\lambda$ [30]. Choosing $y_{\text{ref}}(\cdot) \equiv 0$, $\lambda = 0$, we arrive at the so-called *adaptive stabilization control objective*.

A preferred control strategy is the following [30]:

$$\left.\begin{aligned} e(t) &:= y(t) - y_{\text{ref}}(t)\,, \\ u(t) &= -\Big(k(t)\,e(t) + \kappa\,\tfrac{d}{dt}\big(k(t)\,e(t)\big)\Big)\,, \\ \dot{k}(t) &= \gamma\Big(\max\Big\{0, \big\|\,e(t)\big\| - \lambda\Big\}\Big)^2\,, \end{aligned}\right\} \tag{3}$$

with $k(0) = k_0 \in \mathbb{R}$, $\lambda > 0$, $\kappa = 1$ (just guaranteeing dimensions) and $\gamma \gg 1$.

This controller consists of a very simple feedback mechanism and adaptation law, it is only based on the output of the system and its time derivative - no knowledge of the system parameters is required.

As mentioned in Section I, the biological paradigm vibrissa exhibits two basic modes of operation: a passive and an active mode. Expressing these modes using the presented adaptive control strategies, we conclude that a vibrissa in *passive mode* is a system to be *stabilized* under permanent excitation while enabling to *detect* external extra-perturbations. In an *active mode*, it is to *track* a given oscillatory motion pattern in order to enable the system to recognize, e.g., the surface texture of an external object contacts. Therefore, we can identify these two basic operation modes with

- passive mode: $\lambda$-stabilization (see Fig. 8),

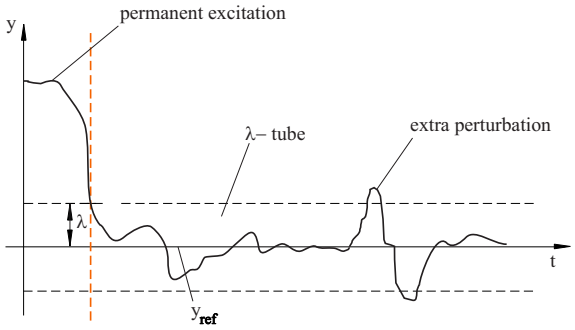


Fig. 8. Vibrissa deflection in passive mode.

- active mode: $\lambda$-tracking (see Fig. 9).

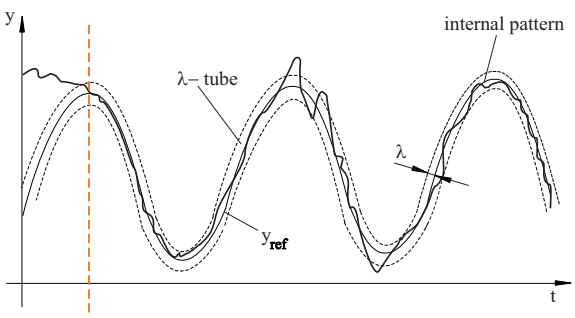


Fig. 9. Vibrissa deflection in active mode.

Note: Because of the randomness of external signals and unknown system parameters, we have to choose the presented adaptive control strategy. The given output of system (1) is $y(t) := \varphi(t)$, hence the equations belong to (2) and the presented controllers achieve their objectives. Now, we apply controller (3) (obviously replacing $u(\cdot)$ by $M_u(\cdot)$) to achieve $\lambda$-stabilization ($y_{\text{ref}}(\cdot) \equiv 0$ in passive mode) and $\lambda$-tracking (in active mode).

## V. Simulations

We point out that the adaptive nature of the controller is expressed by the *arbitrary choice* of the system parameters. Obviously, numerical simulation needs fixed (and known) system data, but the controller *adjusts* its gain parameter *to each set* of system data. Guided by [25], we choose the following parameters (for all simulations, further data will be given on the spot):

- vibrissa: $m = 0.003\,\text{kg}$, $c = 5.7\,\frac{\text{N}}{\text{m}}$, $d = 0.2\,\frac{\text{Ns}}{\text{m}}$, $L = 0.04\,\text{m}$, $a = \frac{L}{10} = 0.004\,\text{m}$, $\big(\varphi(0)\,, \dot{\varphi}(0)\big) = \big(0\,\text{rad}\,, 0\,\frac{\text{rad}}{\text{s}}\big)$;
- environment: $t \mapsto F(t) = \Big(0.1\,\cos(t) + 2\,e^{-(t-20)^2}\Big)\,\text{N}$ (see Fig. 10), which represents a (small) permanent oscillation with a gust of wind; and $g = 9.81\,\frac{\text{m}}{\text{s}^2}$;

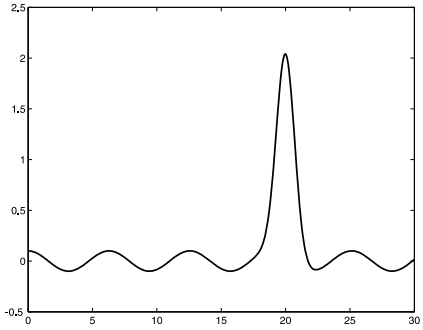


Fig. 10. Excitation $F$ vs. time $t$.

- $\lambda$-tracker: $\lambda = 0.2^\circ \approx 0.064\,\pi$, $\gamma = 50$ (additional parameter to increase the convergence of the controller gain [30]) and $k_0 = 0$.

The following reference signals are used for operation in different modes:

- In the passive mode, the rod motion only needs to be stabilized, therefore it can be simulated with the reference signal (4).

$$t \mapsto \varphi_{ref0}(t) = 0 \tag{4}$$

- The active mode has to be implemented with reference signals performing periodical oscillations enabling the rod to either explore its surroundings or to scan specific objects – and since rodents use two different kinds of oscillations depending on the task, the exploratory and foveal whisking are simulated by two different reference signals. Rodents employ large amplitude sweeps in a low frequency range ($5 - 15$ Hz) to investigate their

environment. As the range of movement of the biological vibrissa amounts to ca. $100^\circ = 1.74$ rad, the amplitude of the exploratory reference signal (5) can be chosen to $A = \frac{1.74}{2} \approx 0.8$ rad. The frequency of the signal $\varphi_{ref1}(t)$ has been set to $f = 5$ Hz according to the findings in [14]. Foveal whisking has been implemented with the reference signal (6), using an amplitude of $A = 0.2$ rad $\approx 12^\circ$ and a frequency of $f = 25$ Hz, since rodents scan specific objects with small amplitude, high frequency movements $(15 - 25$ Hz).

$$t \mapsto \varphi_{ref1}(t) = 0.8 \, \sin(2\,\pi\,5\,t) \tag{5}$$

$$t \mapsto \varphi_{ref2}(t) = 0.2 \, \sin(2\,\pi\,25\,t) \tag{6}$$

### A. Passive mode: $\lambda$-stabilization of $\varphi_{ref0}(\cdot)$

We use controller (3) for stabilization ($y_{\text{ref}}(\cdot) \equiv 0$, rest position to be tracked).

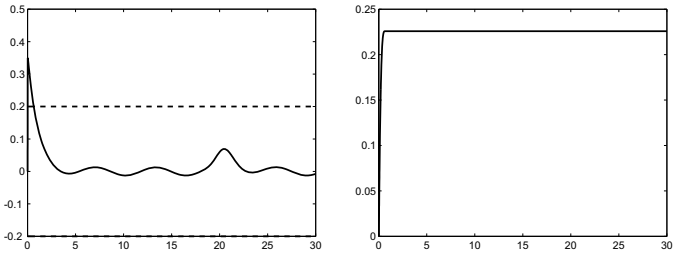

Fig. 11. Output and $\lambda$-strip (left), gain parameter (right), all vs. time $t$.

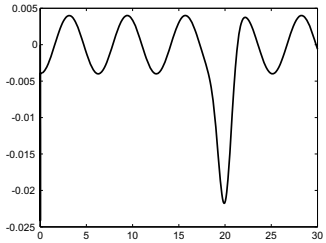

Fig. 12. Control torque $M_u$ vs. time $t$.

Fig. 11 (left) shows a good stabilization, the output is captured by the tube. Fig. 11 (right) shows the convergence of the gain parameter to a constant value, and Fig. 12 the necessary control torque, which reflects the local disturbance around $t = 20$.

### B. Active mode 1: $\lambda$-tracking of $\varphi_{ref1}(\cdot)$

Now, we pass to an active mode. Again, we use controller (3) to track reference signal $\varphi_{ref1}(\cdot)$.

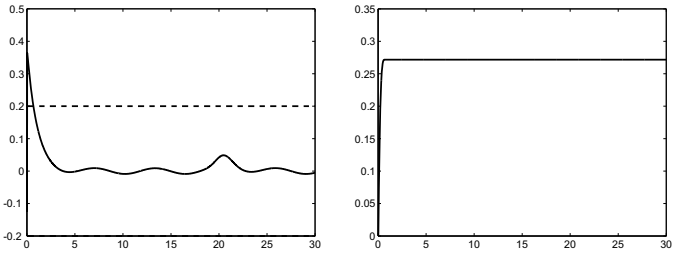

Fig. 13. Error $e$ with $\lambda$-strip (left), and gain parameter $k$ (right), all vs. time $t$.

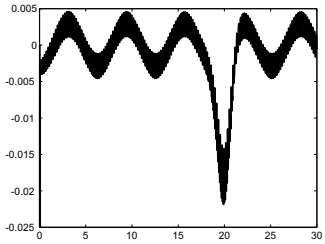

Fig. 14. Control torque $M_u$ vs. time $t$.

We have a good tracking behavior, the output is captured by the tube. This seems to be true because the error is captured by the tube around zero, see Fig. 13 (left). Let us point out that we omit the figure of the output for reasons of presentation (oscillations with high frequency to be tracked) and focus on the error in the following. The controller gain is given in Fig. 13 (right). Fig. 14 shows the control torque that very weakly responds to the local disturbance.

### C. Active mode 2: $\lambda$-tracking of $\varphi_{ref2}(\cdot)$

Here, we simulate another active mode in tracking reference signal $\varphi_{ref2}(\cdot)$ using controller (3).

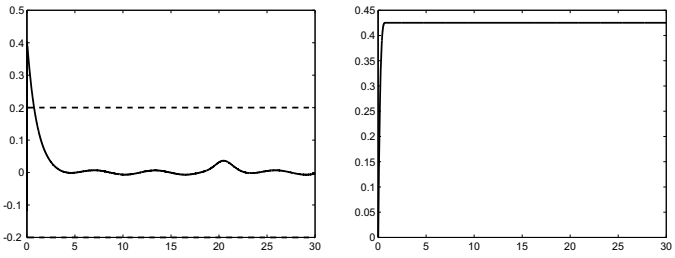

Fig. 15. Error $e$ with $\lambda$-strip (left), and gain parameter $k$ (right), all vs. time $t$.

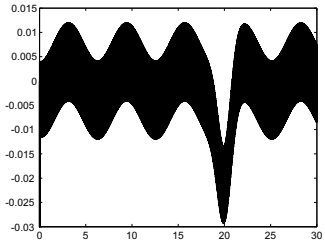

Fig. 16. Control torque $M_u$ vs. time $t$.

Again, and also in simulation of another active mode (foveal whisking), we have a good tracking behavior because the controller works effectively, see Figs. 15 and 16. But, it is quite hard to detect the gust of wind in the system variable. Only the control torque reflects the "peak" around $t = 20\,\mathrm{s}$, see Fig. 16. Therefore, we try to detect the additional excitation by means of other observables.

This problem is tackled in the next section.

## VI. Improved adaptation laws and control schemes

The foregoing simulation shows that the system is not really sensitive to notice the excitation peak around $t = 20$, though tracking and stabilization are essentially guaranteed. Moreover, after the control objective is achieved, the gain parameter still stays at its high value. Figs. 11 (right), 13 (right) and 15 (right) show the monotonic increase of $k(\cdot)$ towards a limit $k_\infty$. But, if some perturbation repeatedly caused the output to leave the $\lambda$-strip, then $k(t)$ would take larger values again and again. The aim is now to avoid this drawback.

At first, we introduce some modifications of the control strategy (3) presented in [1]. These show up with an altered feedback law allowing for output disturbances and various adaptors. Let the control system be of class (2). Then, let us consider controllers of the general form:

$$\left.\begin{aligned} e(t) &:= y(t) - y_{\text{ref}}(t) + n(t)\,, \\ u(t) &= -\Big(k(t)\,e(t) + \kappa\,\tfrac{d}{dt}\big(k(t)\,e(t)\big)\Big)\,, \\ \dot{k}(t) &= f_\lambda(k(t), e(t), t)\,, k(t_0) = k_0 \in \mathbb{R}\,, \end{aligned}\right\} \tag{7}$$

whereby $\lambda > 0$ is the tracking accuracy as in (3). The unknown function $n(\cdot) \in \mathcal{R}$ is a noise corruption of the output, where $\mathcal{R}$ is the set of differentiable functions with absolutely continuous first order derivative and bounded functions and derivatives up to order two, i.e., these functions are elements of $\mathcal{L}^\infty$. It is very important to claim a bound for the output measurement noise signal $n(\cdot)$. This fact is often neglected in literature concerning adaptive tracking control in the presence of noise, see [31]. Further, one can easily see that $\lambda$-tracking only makes sense if the bound of the output measurement noise signal $n(\cdot)$ is smaller than $\lambda$:

$$\big\|n(\cdot)\big\|_\infty < \lambda\,, \tag{8}$$

otherwise the controller cannot distinguish between the reference and noise signal, and so it $\lambda$-tracks the wrong signal $y_{ref}(t) - n(t)$.

Secondly, we apply an improved adaptation law, see [32], that makes $k(\cdot)$ decrease as long as further high lever is not necessary. We distinguish three cases:

1. increasing $k(\cdot)$ while $e$ is outside the tube,
2. constant $k(\cdot)$ after $e$ entered the tube - no longer than a pre-specified duration $t_d$ of stay, and
3. decreasing $k(\cdot)$ after this duration has been exceeded.

For instance:

$$\dot{k}(t) = \begin{cases} \gamma\left(\big\|e(t)\big\| - \lambda\right)^2\,, \text{ if } \big\|e(t)\big\| \geq \lambda\,, \\ 0\,, \text{ if } \Big(\big\|e(t)\big\| < \lambda\Big) \wedge (t - t_E < t_d)\,, \\ -\sigma\,k(t)\,, \text{ if } \Big(\big\|e(t)\big\| < \lambda\Big) \wedge (t - t_E \geq t_d), \end{cases} \tag{9}$$

with given $\sigma > 0$, $\gamma \gg 1$, and $t_d > 0$, whereas the entry time $t_E$ is an internal variable.

Choosing this new adaptor (9) with $\sigma = 0.2$ (moderate exponential decay rate [22]) and $t_d = 1$ (moderate choice of the duration of stay within the $\lambda$-tube [32]), we obtain the following tracking results in an active mode, e.g., $\lambda$-tracking of $\varphi_{ref1}(\cdot)$:

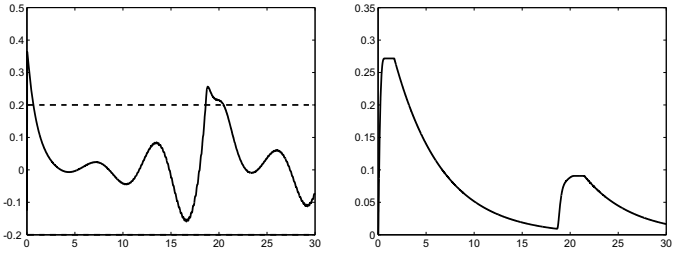


Fig. 17. Error $e$ and $\lambda$-strip (left), and gain parameter $k$ (right), all vs. time $t$.

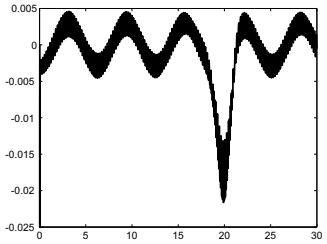


Fig. 18. Control torque $M_u$ vs. time $t$.

The output is forced into the tube, see Fig. 17 (left). The gain $k(\cdot)$ immediately decreases, see Fig. 17 (right), after a $t_d$-stay of $e$ in the tube, see Fig. 17 (left). Apparently, the decrease is too fast: $e$ leaves the tube again but, as a consequence of $\dot{k}$ being proportional to the *square* of the (small) deviation from the $\lambda$-tube, $k$ increases too slowly as to force $e$ quickly back to the tube. The necessary control input is displayed in Fig. 18.

In order to make the attraction of the tube stronger, we use different exponents for large/small distance from the tube, see [32]. For instance:

$$\dot{k}(t) = \begin{cases} \gamma\left(\big\|e(t)\big\| - \lambda\right)^2\,, \text{ if } \big\|e(t)\big\| \geq \lambda + 1\,, \\ \gamma\left(\big\|e(t)\big\| - \lambda\right)^{0.5}\,, \text{ if } \lambda + 1 > \big\|e(t)\big\| \geq \lambda\,, \\ 0\,, \text{ if } \Big(\big\|e(t)\big\| < \lambda\Big) \wedge (t - t_E < t_d)\,, \\ -\sigma\,k(t)\,, \text{ if } \Big(\big\|e(t)\big\| < \lambda\Big) \wedge (t - t_E \geq t_d), \end{cases}$$

with $\sigma\,, \gamma\,, t_d\,, t_E$ as before.

Using this adaptor, we obtain the results from Figs. 19 and 20.

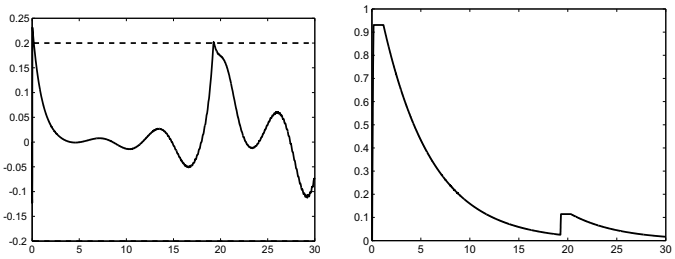

Fig. 19. Error $e$ and $\lambda$-strip (left), and gain parameter $k$, all vs. time $t$.

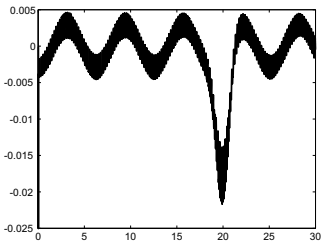

Fig. 20. Control torque $M_u$ vs. time $t$.

Here, one cannot clearly see the advantage of two alternating exponents. The gain parameter $k(\cdot)$ increases very fast in the beginning of the simulation, see Fig. 19 (right). This is due to the "switching on" of the controller. It forces $e$ faster into the tube at cost of a high $k$. Then, $k$ decreases if $e$ stays in the tube for a duration larger than $t_d$, see Fig. 19 (right). The error $e$ is forced back into the $\lambda$-tube very fast, see Fig. 19, because the attraction of the tube is stronger for small deviations $\|e(t)\| - \lambda > 0$. This is on the expense of a tolerable overshooting of $k$ at the beginning, mentioned above. But, interestingly, we are also able to detect solitary excitations in observing the gain $k(\cdot)$ instead of $M_u(\cdot)$, see Fig. 20.

## VII. Conclusions

The foregoing considerations have shown that adaptive control is promising in application to vibrissa systems. In particular, it allows, based on the dynamical equations, to describe two main modes of operation of vibrissae: passive and active ones. More precisely, these control strategies allow the artificial system to proceed its scanning procedure / its mode of operation (e.g., to investigate the surface texture of objects as in [35]) despite the existence of external disturbances — as in nature. Hence, the presented controllers can mimic the adaptive nature of this paragon using adaptive control schemes. Further on, improved adaptive controllers are useful to diminish high gain factors to reduce an overload of the scanning device. As mentioned in this paper, the presented controllers are also robust with respect to output measurement noise.

Therefore, this research on improved controllers should be developed further. Simultaneously, the following problems/tasks are under investigation: separation of an extra receptor from vibrissa to hopefully get more insights into this sophisticated biological system and its data processing, and identification techniques to get knowledge of solitary excitations.

Near future tasks are

- replace the simple model of a circular pendulum by spherical one (to model spatial receptivity),
- tuning of the adaptors (i.e., to find favorable values of $\gamma$, $\sigma$, $t_d$), and investigating rates of convergence,
- hardware experiments to validate the theory,
- to develop elastic vibrissae models, e.g., multi-body systems and/or continuum systems,
- consider a tuft of vibrissae (modeling the intrinsic musculature), not only a single vibrissa.

After doing this, one can think about the application of the presented tracking scenario to replace the kinematic drive/kinematic scanning trail in present application for recognition of object contours and/or texture in, e.g., [33], [34].

## References

[1] C. Behn, M. Scharff, and L. Merker, "Steps towards the Modeling of Animal Vibrissa Modes Using Adaptive Control," in INTELLI 2022 - The Eleventh International Conference on Intelligent Systems and Applications, Venice, Italy, May 2022, pp. 43–49.

[2] M. R. Cutkosky, R. D. Howe, and W. R. Provancher, "Force and Tactile Sensors," in Springer Handbook of Robotics, B. Siciliano and O. Khatib, Eds. Heidelberg: Springer, 2008, pp. 445–476.

[3] T. J. Prescott, M. J. Pearson, B. Mitchinson, J. C. W. Sullivan, and A. Pipe, "Whisking with robots: from rat vibrissae to biomimetic technology for active touch," IEEE Robotics & Automation Magazine, vol. 16, 2009, pp. 42-–50.

[4] A. S. Ahl, "The role of vibrissae in behavior: a status review," Veterinary Research Communications, vol. 10, 1986, pp. 245–268.

[5] M. J. Z. Hartmann, "A night in the life of a rat: vibrissal mechanics and tactile exploration," Annals of the New York Academy of Sciences, vol. 1225, 2011, pp. 110–118.

[6] Y. S. W. Yu, M. M. Graff, and M. J. Z. Hartmann, "Mechanical responses of rat vibrissae to airflow," Journal of Experimental Biology, vol. 219, 2016, pp. 937–948.

[7] S. J. Whiteley, P. M. Knutsen, D. W. Matthews, and D. Kleinfeld, "Deflection of a vibrissa leads to a gradient of strain across mechanoreceptors in a mystacial follicle," Journal of Neurophysiology, vol. 114, 2015, pp. 138–145.

[8] M. Brecht, B. Preilowski, and M. M. Merzenich, "Functional architecture of the mystacial vibrissae," Behavioural Brain Research, vol. 84, 1997, pp. 81–97.

[9] G. E. Carvell and D. J. Simons, "Biometric analyses of vibrissal tactile discrimination in the rat," Journal of Neuroscience, vol. 10, 1990, pp. 2638–2648.

[10] D. Voges et al., "Structural characterization of the whisker system of the rat," IEEE Sensors Journal, vol. 12(2), 2012, pp. 332–339.

[11] A. Schierloh, "Neuronal networks and their plasticity within the barrel cortex of a rat," PhD-Thesis (in German), Technische Universität München, Germany, 2003.

[12] M. Scharff, "Bio-inspired tactile sensing – Analysis of the inherent characteristics of a vibrissa-like tactile sensor," PhD-Thesis, Technische Universität Ilmenau, Germany, 2021.

[13] J. Dörfl, "The musculature of the mystacial vibrissae of the white mouse," Journal of Anatomy, vol. 135, 1982, pp. 147–154.

[14] R. W. Berg and D. Kleinfeld, "Rhythmic whisking by rat: retraction as well as protraction of the vibrissae is under active muscular control," Journal of Neurophysiology, vol. 89, 2003, pp. 104–117.

[15] M. J. Z. Hartmann and J. H. Solomon, "Robotic whiskers used to sense features: Whiskers mimicking those of seals or rats might be useful for underwater tracking or tactile exploration," NATURE, vol. 443, 2006, p. 525.

[16] B. Mitchinson, M. Pearson, C. Melhuish, and T. J. Prescott, "A model of sensorimotor coordination in the rat whisker system," in From Animals to Animats 9: Proc. 9th. Int. Conf. on Simulation of Adaptive Behaviour, 2006, pp. 77–88.

[17] B. Mitchinson, C. J. Martin, R. A. Grant, and T. J. Prescott, "Feedback control in active sensing: rat exploratory whisking is modulated by environmental contact," Proc. R. Soc. B, vol. 274, 2007, pp. 1035–1041.

[18] D. Derdikman et al., "Layer-specific touch-dependent facilitation and depression in the somatosensory cortex during active whisking," The Journal of Neuroscience, vol. 26(37), 2006, pp. 9358–9547.

[19] J. C. Curtis and D. Kleinfeld, "Seeing what the mouse sees with its vibrissae: a matter of behavioural state," Neuron, vol. 50(4), 2006, pp. 524–526.

[20] E. E. Fanselow and M. A. L. Nicolelis, "Behavioral modulation of tactile responses in the rat somatosensory system," The Journal of Neuroscience, vol. 19(17), 1999, pp. 7603–7616.

[21] T. A. Schmitz, "Development and analysis of biologically inspired sensor systems with higher degrees of freedom using the example vibrissa," Master thesis (in German), Technische Universität Ilmenau, Germany, 2011.

[22] C. Behn, "Mathematical modeling and control of biologically inspired uncertain motion systems with adaptive features," Habilitation thesis, Technische Universität Ilmenau, Germany, 2013.

[23] F. A. Lucianna, A. L. Albarracín, S. M. Vrech, F. D. Farfán, and C. J. Felice, "The mathematical whisker: a review of numerical models of rat's vibrissa biomechanics," Journal of Biomechatronics, vol. 49, 2016, pp. 2007–2014.

[24] B. Mitchinson et al., "Empirically inspired simulated electro-mechanical model of the rat mystacial follicle-sinus complex," Proc. R. Soc. Lond., vol. 271, 2004, pp. 2509–2516.

[25] D. Hill, R. Bermejo, P. Zeigler, and D. Kleinfeld, "Biomechanics of the vibrissa motor plant in rat: rhythmic whisking consists of triphasic neuromuscular activity," Journal of Neuroscience, vol. 28, 2008, pp. 3438–3455.

[26] E. Simony et al., "Temporal and spatial charateristics of vibrissa responses to motor commands," Journal of Neuroscience, vol. 30, 2010, pp. 8935–8952.

[27] S. Haiderliu, E. Simony, D. Golomb, and E. Ahissar, "Muscle architecture in the mystacial pad of the rat," The Anatomical Record: Adavances in Integrative Anatomy and Evolutionary Biology, vol. 293, 2010, pp. 1192–1206.

[28] F. G. Barth, "Spider mechanoreceptors," Current Opinion in Neurobiology, vol. 14, 2004, pp. 415–422.

[29] A. N. Kolmogorov and S.V. Fomin, "Elements of the theory of functions and functional analysis," Dover, 1999.

[30] C. Behn, "Adaptive control of straight worms without derivative measurement," Multibody System Dynamics, vol. 26, 2011, pp. 213–243.

[31] A. Ilchmann and E. P. Ryan, "Universal $\lambda$-tracking for nonlinearly-perturbed systems in the presence of noise," Automatica, vol. 30(2), 1994, pp. 337–346.

[32] C. Behn, "Modeling, analysis and control of mechanoreceptors with adaptive features," Informatics in Control, Automation and Robotics – Lecture Notes in Electrical Engineering (LNEE), vol. 325, J.-L. Ferrier et al. Eds., Springer International Publishing Switzerland, 2014, pp. 349–366.

[33] M. Scharff, J. H. Alencastre, and C. Behn, "Detection of surface texture with an artificial tactile sensor," Interdisciplinary Applications of Kinematics – Mechanisms and Machine Science, vol. 71, A. Kecskeméthy et al. Eds., Cham: Springer, 2019, pp. 43–50.

[34] L. Merker, M. Scharff, K. Zimmermann, and C. Behn, "Surface Sensing of 3D Objects Using Vibrissa-like Intelligent Tactile Sensors," Proceedings INTELLI 2020: The Ninth International Conference on Intelligent Systems and Applications, Porto (Portugal), IARIA, 2020, pp. 18–23.

[35] M. Scharff, "Bio-Inspired Tactile Sensing: Distinction of the Overall Object Contour and Macroscopic Surface Features," Perspectives in Dynamical Systems I: Mechatronics and Life Sciences, Springer Proceedings in Mathematics & Statistics, vol 362, J. Awrejcewicz et al. Eds., Cham: Springer, 2022, pp. 107–117.